Morphology effect on the electrochromic and electrochemical performances of NiO thin films

X.H. Xia[a], J.P. Tu[a,*], J. Zhang[a], X.L. Wang[a], W.K. Zhang[b], H. Huang[b]

[a] Department of Materials Science and Engineering, Zhejiang University, Hangzhou 310027, China
[b] College of Chemical Engineering and Materials Science, Zhejiang University of Technology, Hangzhou 310032, China

ARTICLE INFO

ABSTRACT

NiO thin films on ITO substrate were prepared by chemical bath deposition (CBD) and sol–gel method, respectively. The microstructure and morphology of the NiO films were characterized by X-ray diffraction (XRD) and scanning electron microscopy (SEM). Both the films have polycrystalline cubic NiO, but have distinct morphology. The CBD NiO thin film with a highly porous structure exhibited a noticeable electrochromic performance. The variation of transmittance was high up to 82% at 550 nm and the coloration efficiency (CE) was calculated to be 42 cm^2 C^{-1}. The sol–gel NiO thin film with a smoothly compact structure presented 35% and 28 cm^2 C^{-1} at 550 nm, respectively. The electrochemical properties of both the NiO thin films were investigated in 1 M KOH electrolyte by means of cyclic voltammetry (CV) and electrochemical impedance spectroscopy (EIS) measurements. The CV and EIS measurements revealed that the CBD NiO thin film had better electrochemical reversibility, higher reactivity and reaction kinetics due to its highly porous structure.

© 2008 Elsevier Ltd. All rights reserved.

1. Introduction

The electrochromic material is able to sustain reversible and persistent changes of its optical properties upon the application of a voltage [1]. Transition metal oxides such as WO$_3$ [2], NiO [3], MoO$_3$ [4], IrO$_3$ [5] are widely studied as the electrochromic materials. Among these transition metal oxides, nickel oxide is an attractive material due to its high coloration efficiency (CE), large dynamic range, good cyclic reversibility and low material cost [6]. NiO can be used as a counter electrode to WO$_3$ electrode in smart window, where the optical modulation increases due to the simultaneous modulation of both electrodes [7,8]. A variety of methods have been used to prepare the electrochromic NiO thin films, such as sputtering [9], chemical vapor deposition [10], electro-deposition process [11], pulsed laser deposition [12], spray pyrolysis [13], sol–gel process [14] and chemical bath deposition (CBD) [15], etc. Among these methods, the chemical bath deposition and sol–gel processes have many advantages of low cost, low temperature and easy to be large-area prepared.

The morphology characteristic should be taken into careful consideration since the electrochromic and electrochemical performances of NiO thin film are tightly related to its morphology.

However, few investigations have been done on the morphology effect on the electrochromic and electrochemical performances of the NiO thin film. The polycrystalline NiO thin films prepared by sputtering [16], pulsed laser deposition [17] and spray pyrolysis [13] often showed the compact structure associated with rough appearance or large grains and exhibited low efficiency of electrochromism. Moreover, even the NiO thin films prepared by the same technique could exhibit distinct morphologies and electrochromic performance. The electro-deposited polycrystalline NiO thin films prepared by Wu and Yang [18] had a highly porous structure and exhibited high transmittance variation up to 80% at 550 nm, while the electro-deposited polycrystalline NiO thin films obtained by Uplane et al. [11] showed a compact structure with spherical grains and had low transmittance modulation. This distinction indicates that the morphology do influence the electrochromic performance of the NiO thin films. In this present work, two NiO thin films with distinct morphology were prepared by chemical bath deposition and sol–gel method. The relationship between the morphology and the electrochromic and electrochemical properties of NiO thin films were investigated.

2. Experimental

The CBD NiO thin film was deposited on indium tin oxide (ITO) substrate with a size of 2.5 × 2.5 cm^2. Solution for chemical bath deposition was obtained by mixing 80 ml of 1 M nickel sulfate,

60 ml of 0.25 M potassium persulfate and 20 ml of aqueous ammonia (25–28%) in a 250 ml Pyrex beaker under magnetic stirring at room temperature. Before deposition, the ITO substrate was cleaned ultrasonically in ethanol and acetone for 15 min, respectively, and then placed vertically in the beaker. After stirring for 10 min, the substrate was removed from the solution and washed with distilled water. Afterwards, the as-prepared sample was dried at 75 °C, and then annealed at 300 °C for 1.5 h. The thickness of the annealed film was approximately 210 nm, determined with an Alpha-step 200 profilometry.

In comparison with the NiO thin film prepared by chemical bath deposition, the NiO thin film was also prepared by sol–gel process. Nickel acetate tetrahydrate ($Ni(CH_3COO)_2 \cdot 4H_2O$) was used as the starting material for Ni sols. A precursor solution was prepared by dissolving 12.4 g nickel acetate salt in a mixture of ethanol, 1-butanol and ethylene glycol. The resulting solution was refluxed for 3 h under continuous stirring at 75 °C. Then a predetermined amount of water was added to the solution, and the solution was refluxed for another 1 h. After the solution was allowed to cool at room temperature, an aqueous solution of polyvinyl alcohol (PVA) was added in order to improve adherence and abrasion resistance [19]. The sol was coated on the conductive side of the ITO substrate by spin coating, where the substrate was spun at 2500 rpm for 30 s on a spinner. Afterwards, the precursor film was dried in air at room temperature, and then annealed at 300 °C in air for 1.5 h. The thickness of the annealed film was approximately 200 nm depending on solution viscosity, which could be adjusted by PVA addition.

The morphology and microstructure of the annealed films were characterized by a field emission scanning electron microscopy (FESEM, Hitachi S-4700), X-ray diffraction (XRD, Philips PC-APD with Cu Kα radiation).

The transmission spectra of NiO thin films in the fully colored and fully bleached states were measured over the range from 200 to 900 nm with a SHIMADZU UV-240 spectrophotometer. Each spectrum was recorded ex-situ (after the samples taken out of the three-compartment system, instantly rinsed and wiped off from the remaining persistent water). The cyclic voltammetry (CV) and electrochemical impedance spectroscopy (EIS) measurements were carried out in a three-compartment system containing 1 M KOH as electrolyte, Hg/HgO as reference electrode and a nickel mesh as counter-electrode. Cyclic voltammetry measurements of NiO films were performed using a CHI660B electrochemical workshop with a scanning rate of 10 mV s^{-1} between 0.2 V and 0.65 V at room temperature (25 ± 1 °C). The NiO film electrodes with 0.5×1.0 cm^2 in sizes were used for electrochemical impedance spectroscopy measurements, which were made with a superimposed 5 mV sinusoidal voltage in the frequency range of 100 kHz–0.01 Hz. The EIS obtained experimentally were analyzed using a nonlinear least squares fitting program EQUIVCRT.

3. Results and discussion

Fig. 1 shows the XRD patterns of both NiO films deposited on ITO substrate, respectively. The diffraction peaks of both the samples can be indexed as cubic NiO phase (JCPDS 4-0835). The SEM images of both the NiO films are shown in Fig. 2. It is observed that the CBD NiO thin film has a structure with huge porosity, which is similar to that reported by Wu and Yang [18]. The NiO thin film prepared by sol–gel process exhibits a compact and highly homogeneous surface morphology.

The electrochromic properties of the NiO thin films were measured after the film electrodes had been subjected to cyclic voltammetric test for 10 cycles in 1 M KOH solution. The NiO film electrodes were colored by applying step voltages of 0.65 V for coloration and 0.2 V (vs. Hg/HgO) for bleaching. The color of the
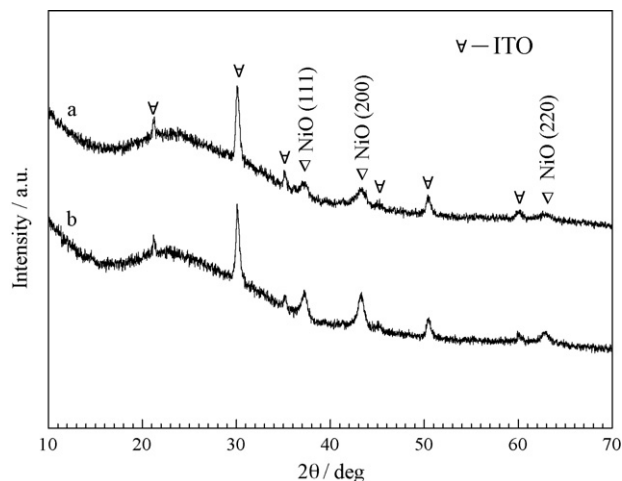

Fig. 1. XRD patterns of NiO films deposited on ITO substrate: (a) CBD NiO film, (b) sol–gel NiO film.

NiO thin films changes from brown (colored state) to transparent (bleached state). Fig. 3 shows spectral transmittance of both the NiO films in the colored and bleached states. It is clearly seen that the CBD NiO thin film exhibits much better transmittance modulation than the sol–gel NiO thin film. The transmittance variation of CBD NiO thin film is high up to 82% at 550 nm, which is comparable with the result obtained by Wu and Yang [18], while the sol–gel NiO thin film only presents 35% at 550 nm.
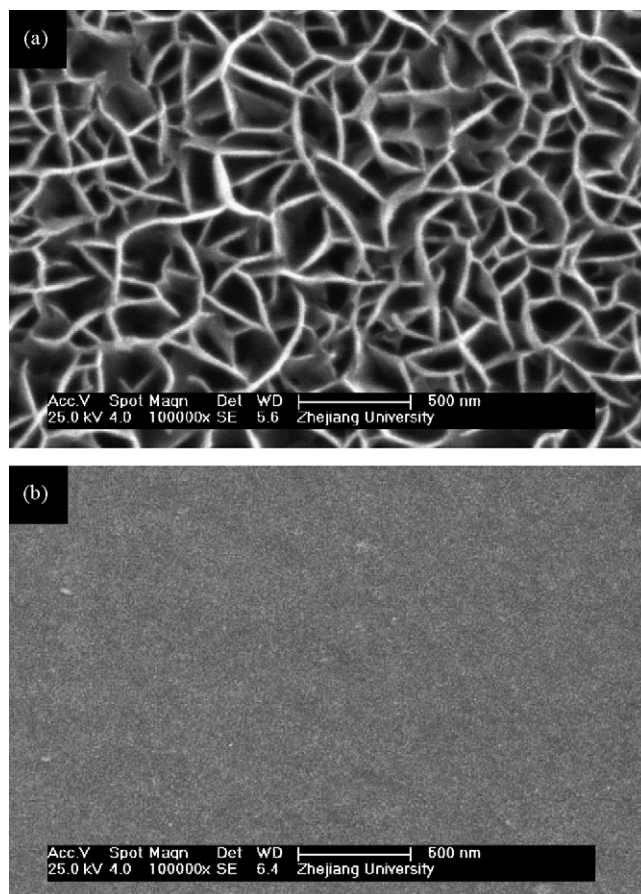

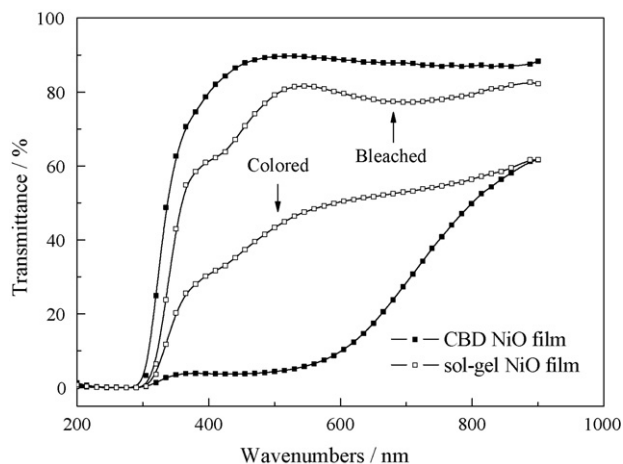**Fig. 2.** SEM micrographs of (a) CBD NiO film, (b) sol–gel NiO film.

Fig. 3. Optical transmittance spectra of NiO films.

Fig. 4. Cyclic voltammograms of NiO film electrodes in the potential region of 0.2–0.65 V at a scanning rate of 10 mV s^{-1} at the 10th cycle.

The coloration efficiency is a useful figure of merit for the comparison of various electrochromic materials. η, which designates the value of CE, is defined as the ratio of change of optical density (ΔOD) of the film in its colored (T_c) and bleached (T_b) state at a certain wavelength and corresponding injected (or ejected) charge density (Q) per unit area. The change of optical density is obtained as follows:

$$\eta(\lambda) = \frac{\Delta OD(\lambda)}{Q} \tag{1}$$

$$\Delta OD(\lambda) = \log\frac{T_b}{T_c} \tag{2}$$

In this work, the value of CE of the CBD NiO thin film is calculated to be about 42 cm^2 C^{-1} at 550 nm. This value is comparable with those obtained from amorphous nickel oxide thin films grown by CVD (44 cm^2 C^{-1}) [10] and electro-deposition (42 cm^2 C^{-1}) [20], but much higher than other polycrystalline NiO thin films by laser pulsed deposition [17], spray pyrolysis [21] and sol–gel process [22]. The value of CE of the sol–gel NiO film is calculated about 28 cm^2 C^{-1}, much lower than that of the CBD NiO film. It suggests that the higher value of CE for the CBD NiO film is mainly due to the highly porous structure. It has been pointed out that the coloration (bleaching) reaction is a double injection (extraction) of ions and electrons to (from) the film. The processes are believed to firstly occur at grain boundaries and on grain surfaces [23]. The highly porous structure of NiO film provides large reaction surface and inner space. It also facilitates electrolyte soaking into the particles and shortens the proton diffusion paths within the bulk of NiO. Meanwhile, the intercrossing network provides much more paths for the double injection (extraction) of ions and electrons to (from) the film [18]. All these contribute to the improvement of electrochromic performance. Moreover, a compact film may be too dense for ion intercalation, thus it will result in low electrochromic performance.

Fig. 4 presents typical cyclic voltammograms of both NiO film electrodes in the potential region of 0.2–0.65 V at a scanning rate of 10 mV s^{-1}. Just one redox process is seen in the CV curve. The coloration process of the film is associated with the oxidation peak appearing before the oxygen evolution reaction (OER), which can be attributed to the following electrochemical reactions [24–26]:
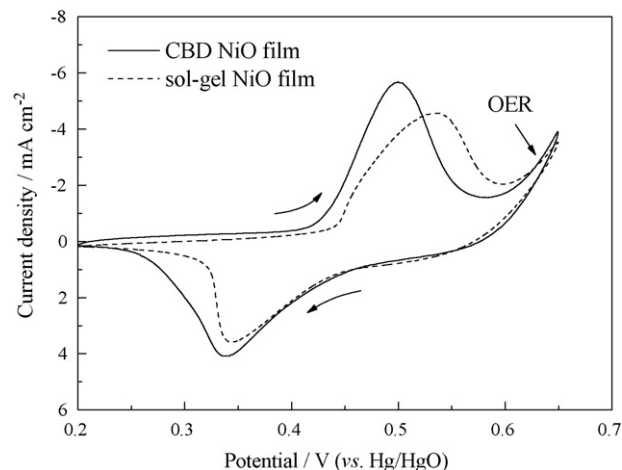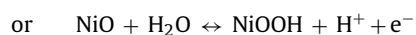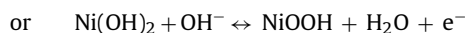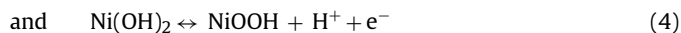
$$NiO + OH^- \leftrightarrow NiOOH + e^- \tag{3}$$

$$\text{or} \quad NiO + H_2O \leftrightarrow NiOOH + H^+ + e^-$$

The bleaching process is associated with the reduction peak, which can be attributed to the following electrochemical reactions:

$$\text{and} \quad Ni(OH)_2 \leftrightarrow NiOOH + H^+ + e^- \tag{4}$$

$$\text{or} \quad Ni(OH)_2 + OH^- \leftrightarrow NiOOH + H_2O + e^-$$

It is seen that extraction of protons and electrons from the film leads to coloration and an insertion of protons and electrons into the film leads to the bleaching. The experiment results describing the features of the voltammograms are listed in Table 1 in detail. As shown in Table 1, the CBD NiO thin film shows much lower oxidation potential than the sol–gel NiO thin film in the same state. Furthermore, the CBD NiO thin film shortens the potential separation between the oxidation peak and the reduction peak. It is well-known that the peak potential separation is used as a measure of reversibility. It indicates that the CBD NiO thin film has better reaction reversibility. In addition, the cathodic and the anodic peak currents of the CBD NiO thin film are much higher than those of the sol–gel NiO thin film, indicating that the CBD NiO thin film has much higher electrochemical activity.

Fig. 5 shows the EIS plots of NiO thin films after the film electrodes had been subjected to cyclic voltammetric test for 10 cycles. As seen in this figure, the impedances of both the NiO film electrodes all consist of a depressed arc in high frequency regions and a straight in low frequency regions. Generally, the semicircle reflects the electrochemical reaction impedance of the film electrode and the straight line indicates the diffusion of the electroactive species. The sol–gel NiO thin film exhibits a much larger capacitive arc and higher slope than the CBD NiO thin film. According to former reports [27,28], the bigger semicircle means the larger charge-transfer resistance, and the higher slope signifies the lower diffusion rate. It is concluded that the CBD NiO thin film has the lower charge transfer resistance and ion diffusion resistance.

Table 1
Characteristics parameters for the cyclic voltammograms of both NiO film electrodes (corresponding to Fig. 4)

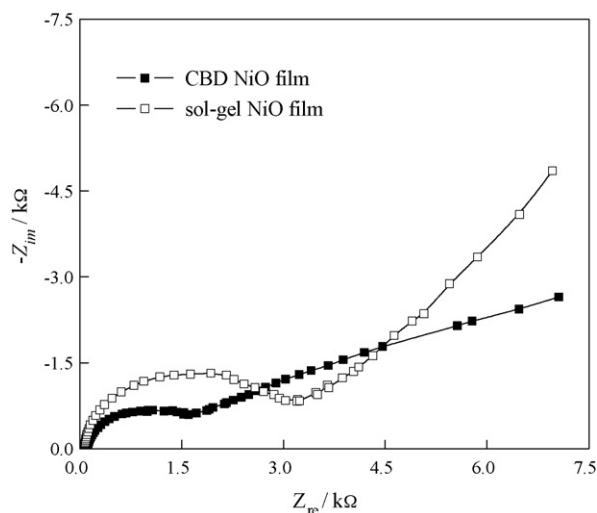| Film electrode	Anode peak potential (mV)	Cathode peak potential (mV)	Peak potential separation (mV)
CBD NiO film	499	342	157
Sol–gel NiO film	535	344	191

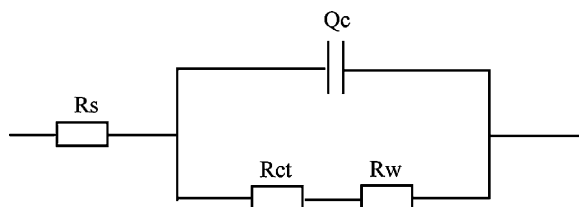**Fig. 5.** EIS plots of both NiO film electrodes.

Fig. 6. Equivalent circuit of NiO film electrode.

Table 2
EIS parameters of both NiO film electrodes

Film electrode	R_{CT} (kΩ)	Z_W (kΩ)	Q_C (F)
CBD NiO film	1.81	0.37	0.26
sol–gel NiO film	2.85	0.66	0.09

The equivalent circuit of the NiO thin film electrode, which can be expressed by Central Digital Computer (CDC) code as R_S (Q_C ($R_{CT}Z_W$)), is also shown in Fig. 6. R_S, Q_C, R_{CT} and Z_W, designate the total ohmic resistance of solution and electrodes, the capacitance of the double layer, the electrochemical reaction impedance and the Warburg impedance, respectively. These parameters can be calculated through the plots shown in Fig. 5 with ZView software. Some values are listed in Table 2 except the total ohmic resistance of solution and electrodes. The total ohmic resistance obtained in three-electrode system does not have much meaning.

According to the reports on the EIS of Ni(OH)$_2$ electrodes, the semicircle, which represents an electrochemical process occurring at the double layer of the electrode, is influenced by the actual surface area of the active material [29]. As shown in Table 2, the value of Qc of the sol–gel NiO thin film is much lower than that of the CBD NiO thin film. It can be inferred that the CBD NiO thin film has much larger reaction surface than the sol–gel thin film. The values of R_{CT} and R_W of the CBD NiO thin film are lower than those of the sol–gel NiO thin film, indicating that the porous structure is more favorable for charge transfer and ion diffusion than the compact structure, then resulting in higher reactivity and reaction kinetics.

4. Conclusion

NiO thin films were prepared by chemical bath deposition and sol–gel method, respectively. The highly porous CBD NiO thin film exhibited much better electrochromism compared to the smoothly compact sol–gel NiO thin film. The CBD NiO thin film exhibited a variation of transmittance up to 82% at 550 nm and the coloration efficiency was calculated to be 42 cm^2 C^{-1}, while the sol–gel NiO thin film only presented 35% and 28 cm^2 C^{-1} at 550 nm, respectively. The CV and EIS measurements revealed that the CBD NiO film electrode showed better electrochemical reversibility, higher reactivity and reaction kinetics.

References

[1] C.G. Granqvist, E. Avendano, A. Azens, Thin Solid Films 442 (2003) 201.
[2] Maria Hepel, Haley Redmond, Indeewari Dela, Electrochim. Acta 52 (2007) 3541.
[3] I. Bouessay, A. Rougier, P. Poizot, J. Moscovici, A. Michalowicz, J.M. Tarascon, Electrochim. Acta 50 (2005) 3737.
[4] Tarsame S. Sian, G.B. Reddy, Electrochim. Acta 49 (2004) 5223.
[5] H. Elzanowska, E. Miasek, V.I. Birss, Electrochim. Acta 53 (2008) 2706.
[6] C.G. Granqvist, Adv. Mater. 15 (2003) 1789.
[7] C.G. Granqvist, J. Eur. Ceram. Soc. 25 (2005) 2907.
[8] E. Avendano, L. Berggren, G.A. Niklasson, C.G. Granvist, A. Azens, Thin Solid Films 496 (2006) 30.
[9] Y. Zhou, D.H. Gu, Y.Y. Geng, F.X. Gan, Mater. Sci. Eng. B 135 (2006) 125.
[10] T. Maruyama, S. Arai, Sol. Energy Mater. Sol. Cells 30 (1993) 257.
[11] M.M. Uplane, S.H. Mujawar, A.I. Inamdar, P.S. Shinde, A.C. Sonavane, P.S. Patil, Appl. Surf. Sci. 253 (2007) 9365.
[12] N. Penin, A. Rougier, L. Laffont, P. Poizot, J.M. Tarascon, Sol. Energy Mater. Sol. Cells 90 (2006) 422.
[13] B.A. Reguig, A. Khelil, L. Cattin, M. Morsli, J.C. Bernede, Appl. Surf. Sci. 253 (2007) 4330.
[14] E. Ozkan Zayim, I. Turhan, F.Z. Tepehan, N. Ozer, Sol. Energy Mater. Sol. Cells 92 (2008) 164.
[15] S.Y. Han, D.H. Lee, Y.J. Chang, S.O. Ryu, T.J. Lee, C.H. Chang, J. Electrochem. Soc. 153 (2006) 382.
[16] S.R. Jiang, B.X. Feng, P.X. Yan, X.M. Cai, S.Y. Lu, Appl. Surf. Sci. 174 (2001) 125.
[17] L. Bouessay, A. Rougier, B. Beaudoin, J.B. Leriche, Appl. Surf. Sci. 186 (2002) 490.
[18] M.S. Wu, C.H. Yang, Appl. Phys. Lett. 91 (2007) 033109.
[19] A. Surca, B. Orel, J. Sol–Gel Sci. Tech. 8 (1997) 743.
[20] S.A. Mahmoud, S.A. Aly, M. Abdel-Rahman, K. Abdel-Hady, Physica B 293 (2000) 125.
[21] J. Arakaki, R. Reyes, M. Horn, W. Estrada, Sol. Energy Mater. Sol. Cells 37 (1995) 33.
[22] J.Y. Park, K.S. Ahn, Y.C. Nah, H.S. Shim, J. Sol–Gel Sci. Tech. 31 (2004) 323.
[23] J. Nagai, Sol. Energy Mater. Sol. Cells 31 (1993) 291.
[24] S.I. Cordoba-Torressi, A. Hugot-Le Goff, S. Joiret, J. Electrochem. Soc. 138 (1991) 1554.
[25] M. Chigane, M. Ishikawa, J. Electrochem. Soc. 141 (1994) 3439.
[26] C. Natarajan, H. Matsumoto, G. Nogami, J. Electrochem. Soc. 114 (1997) 121.
[27] A.H. Zimerman, P.K. Effa, J. Electrochem. Soc. 131 (1984) 709.
[28] R.D. Armstrong, H. Wang, Electrochim. Acta 36 (1991) 759.
[29] Y.H. Xu, Int. J. Hydrogen Energy 29 (2004) 749.